COMPDYN 2023
9th ECCOMAS Thematic Conference on
Computational Methods in Structural Dynamics and Earthquake Engineering
M. Papadrakakis, M. Fragiadakis (eds.)
Athens, Greece, 12-14 June 2023

DYNAMIC AMPLIFICATION OF TRAFFIC LOADS ON ROAD BRIDGES EVALUATED USING PROBABILISTIC TRAFFIC SIMULATIONS

Marian Ralbovsky[1], Maciej Kwapisz[1], Alois Vorwagner[1] and Stefan Lachinger[1]

[1] AIT Austrian Institute of Technology
Center for Low-Emission Transport
Giefinggasse 4, 1210 Vienna, Austria
{marian.ralbovsky, maciej.kwapisz, alois.vorwagner, stefan.lachinger}@ait.ac.at

Abstract

The traffic loads on road bridges undergo long-term changes as the transport requirements and vehicle technologies develop over time. The current traffic load models of Eurocode were developed decades ago. With the growing database of available axle-load measurements, a re-evaluation seems technically possible. However, dynamic amplification factors need to be determined additionally to the quasi-static load effects.
The presented work is based on calculating the effects of simulated traffic flows on a set of chosen bridges. The traffic was generated using probabilistic traffic simulations, which consider different traffic intensities and a combination of probabilistic and deterministic traffic/vehicle parameters. In this work, 20 years of traffic flow was generated and applied on chosen simple bridge models of single-span bridges with spans ranging from 15 to 120 m. Dynamic Amplification Factors were calculated for all significant traffic events.
The results showed that DAF has a decreasing tendency with increasing quasi-static load effects, which was also observed in previous evaluations from monitoring data. Further observed tendencies were decreasing DAF with increasing span length and increasing DAF with decreasing bridge mass per unit length.

Keywords: Road bridge, Dynamic amplification, Traffic simulation, Axle loads, DAF.

1 INTRODUCTION

The amplification of traffic-induced loads on road bridges occurs due to dynamic effects of the coupled bridge-vehicle system. The amplitude of the amplification is influenced by the vehicle dynamics, road roughness profile and most prominently by dynamic bridge properties and its resonance behavior. Unlike for railway bridges, the Eurocode [1] does not specify the values of the dynamic amplification on road bridges. Instead, the dynamic effects are already included in the load models for the ULS (Ultimate Limit State), which were established assuming medium pavement quality (road surface class C in [1], Annex B) and a pneumatic vehicle suspension. In case of fatigue load models, the Eurocode assumes pavement of good quality (road surface class B) for dynamic effects that are included in the load models and specifies an additional dynamic amplification factor $\Delta\varphi_{fat}$ to be taken into account near expansion joints. This additional factor reaches values up to 1.3 (at the joint) but diminishes quickly to value of 1.0 at 6 m distance from the joint.

In the last 10-20 years, the amount of available data on actual traffic loads increased significantly due to installation and operation of Weigh-In-Motion (WIM) systems, which measure axle loads and distances in flowing traffic at different locations across Europe. The new data cluster gives an opportunity for new evaluations of road traffic models. Further, future traffic scenarios are being considered. For example, the EU-project LEVITATE investigated the effects of automated driving. Among other aspects, the impacts of truck platooning on bridges were analyzed [2]. These new evaluations, which primarily concentrate on quasi-static load effects, need to additionally consider also the dynamic amplification of traffic loads.

For this purpose, the Dynamic Amplification Factor (DAF) is a widely used quantity. The DAF for a quantity X (which can be for example bending moment, shear force, stress) is defined as the ratio of the maximum of total response X_{tot} and the maximum of quasi-static response X_{stat} (1).

$$DAF(X) = \frac{max(X_{tot})}{max(X_{stat})} \tag{1}$$

It was observed, both in measurements and in simulation results, that the value of DAF has decreasing trend with increasing gross weight of passing vehicles. Kalin et.al. [3] presented evaluation of the DAF at different percentiles of the occurring vehicle weights on Slovenian motorways and state roads, as well as on US highways. In here, the linear regression of DAF_p curves resulted in approx. halving of the value of DAF when comparing DAF at maximum recorded loading to mean DAF.

The evaluation of the DAF from measurements is often possible using simple signal-processing techniques, which filter-out the dynamic components. Figure 1 shows an evaluation of DAF from strain measurements acquired on an Austrian highway bridge. The strain gauge was placed in midspan of a concrete box-girder bridge with multiple spans. The figure displays data from more than 1 year of continuous monitoring, and each dot represents an evaluated DAF from one traffic event. In here, the weight of the passing vehicles was not evaluated, thus the horizontal axis represents the amplitude of the measured quasi-static strain (peak-to-peak) instead, which is a direct effect of axle weights on the bridge. The decreasing trend of the DAF is also here apparent.

The fact that values of DAF are lower for traffic events with high quasi-static load is beneficial for the evaluation of total load extremes.

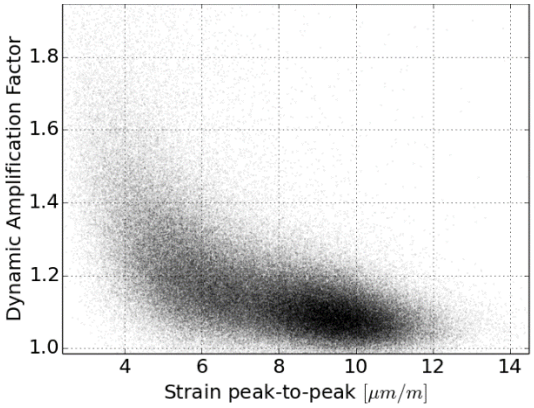

Figure 1: DAF of strain in midspan evaluated from measurements at an Austrian highway bridge

O'Brien et.at. [4] argued that the Assessment Dynamic Ratio (ADR) is a more representative quantity than DAF. The ADR is defined as the ratio of characteristic values of the total effect $\tilde{X}_{tot}$ and of the quasi-static effects $\tilde{X}_{stat}$ (2). While DAF can be evaluated for each traffic event separately, the ADR is evaluated only once for the whole traffic flow, because the statistical evaluation is included in the separate evaluations of $\tilde{X}_{tot}$ and $\tilde{X}_{stat}$.

$$ADR(X) = \frac{\tilde{X}_{tot}}{\tilde{X}_{stat}} \tag{2}$$

The research of comparing DAF and ADR was continued by Carey et.al. [5], concluding that ADR is a more reliable value, especially when evaluating extreme values of traffic loads.

The work presented here intends to investigate DAF using numerical simulations. It builds on the traffic load simulations, which were performed during the finished project LEVITATE, and further extended in the currently ongoing project REAL-LAST.

2 SIMULATION METHOD AND PARAMETERS

2.1 Traffic

Traffic flows were generated using existing traffic simulation algorithms. These result in a simulated sequence of vehicles and include a complete description of the vehicle sequences: vehicle types, their masses and distances, which are then decomposed into axle sequences for each lane. An axle sequence consists of axle forces and their distances. Although the traffic simulation algorithm contains also the formation of congestions, they are not relevant for dynamic amplification evaluations. Therefore, only flowing traffic was analyzed dynamically.

The traffic simulation adopted following assumptions:

- Traffic is a random stationary process and does not evolve over time
- Vehicle speed is constant and all vehicles in one lane share the same speed
- Vehicles do not change lanes while on the bridge
- Most vehicles comply with the prescribed limits of gross vehicle weight; violations of this limit are not excessive
- The distribution of the vehicle amount on a two-lane highway is assumed as 80%-20% until the capacity of the right lane is saturated.

Vehicle properties (Figure 2) as well as traffic composition (Table 1) were adopted from [6]. The traffic flows consists of personal cars and 5 truck types. The right lane is occupied by trucks

only, simulating an inter-city highway traffic. The truck types include two 5-axle trucks (types 41 & 98), two 4-axle trucks (types 33 & 97) and one 2-axle truck (type 8). Special vehicles, like a crane vehicle (mass of which is displayed in Figure 2 left) were not considered in the modelled traffic mix.

Lane	Type 8	Type 33	Type 41	Type 97	Type 98	Cars
Right	11 %	5 %	17 %	8 %	59 %	0 %
Left	2.20 %	1 %	3.40 %	1.60 %	11.80 %	80 %

Table 1: Traffic composition

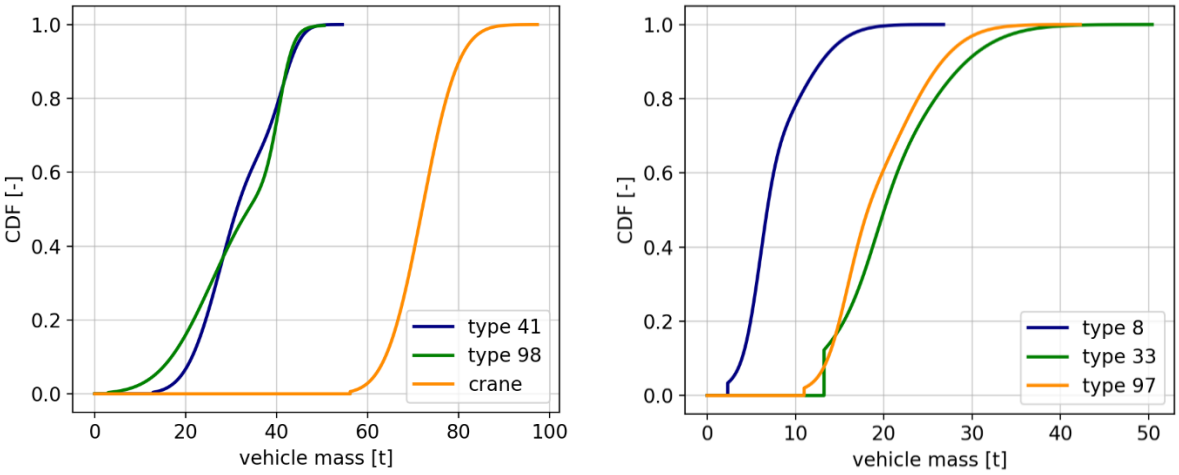

Figure 2: Cumulative distributions of gross vehicle masses for simulated truck types

The traffic was modelled to have two lanes. The generation of vehicle sequence is a random process with the above listed properties. Axle distances as well as the distribution of total vehicle weight to individual axles were assumed to be constant for each vehicle type. These vehicle properties were also adopted from [6].

Different traffic situations were simulated, with traffic volumes ranging from 12.000 vehicles/day to 120.000 vehicles/day. The initial assumption of having 80% of the vehicles in the right lane could be sustained up to a traffic volume of 38.000 vehicles/day. At this point, the right lane became saturated and part of the vehicles from right lane were assumed to start switching to the left lane, thus gradually changing composition of the left lane with increasing traffic volume.

The vehicle distances followed a lognormal distribution. The shape and scale of the distribution was fitted to match the modelled traffic volume, assuming a vehicle speed of 80 km/h.

In total, 20 years of traffic was generated.

2.2 Bridges

The population of simulated bridges consisted of 35 bridges, properties of which are listed in Table 2. The bridge set includes most common bridge types: reinforced-concrete slab, prestressed-concrete T-beam, prestressed-concrete box-girder, composite bridge with welded steel girders, composite bridge with steel box-girders, steel girder bridge with orthotropic deck, and steel box-girder bridge. The cross-section dimensions were estimated based on common construction and dimensioning rules. All bridges were assumed to carry a two-lane highway, thus the deck width was modelled with 10.5 m.

Bridge type	Span [m]	μ [t/m]	f_0 [Hz]	Bridge type	Span [m]	μ [t/m]	f_0 [Hz]
RC slab	15	29.4	5.65	Comp.girder	30	11.6	2.7
RC slab	15	22.8	4.17	Comp.girder	35	11.8	2.4
RC slab	20	38.2	4.3	Comp.girder	40	12	2.15
RC slab	20	29.4	3.18	Comp.girder	50	12.5	1.8
PC T-beam	20	16.8	5.83	Comp.box-girder	40	13.4	2.05
PC T-beam	20	14.9	3.77	Comp.box-girder	50	14	1.75
PC T-beam	25	19.2	4.78	Comp.box-girder	60	14.5	1.52
PC T-beam	25	16.7	3.17	Comp.box-girder	70	15	1.35
PC T-beam	30	21.6	4.04	Steel girder	35	6.1	2.61
PC T-beam	30	18.4	2.72	Steel girder	40	6.3	2.4
PC T-beam	35	24	3.49	Steel girder	50	6.6	2.08
PC T-beam	35	20.1	2.38	Steel girder	60	6.9	1.84
PC T-beam	40	26.4	3.07	Steel box-girder	70	7	1.73
PC T-beam	40	21.9	2.1	Steel box-girder	90	7.7	1.44
PC box-girder	40	21.1	3.2	Steel box-girder	120	9	1.14
PC box-girder	50	23.7	2.57				
PC box-girder	60	26.8	2.12				
PC box-girder	70	30.4	1.8				
PC box-girder	90	37.1	1.38				

Table 2: Basic properties of simulated bridges

Due to large amount of performed simulations, a simple bridge model was required in order to keep the calculation performant. Therefore, bridges were simulated as simply-supported single-span beams, effectively neglecting torsional effects of the two-lane traffic. Multi-span bridges are expected to produce lower dynamic amplifications, therefore this assumption is deemed to be conservative.

2.3 Calculation

The calculation was carried out by means of transient dynamic analysis using the mode superposition method. The traffic loads were modeled as moving axle forces. The analysis does not contain any vehicle dynamics, nor effects of road roughness. Each axle force is constant in time. Therefore, the dynamic behavior arises solely from the bridge structure.

To reduce the computational effort, the traffic flow was filtered for the largest traffic events. First, a quasi-static simulation was performed and for each month of traffic, 100 traffic events that produced the highest quasi-static bridge response were selected. This was done separately for the midspan bending moment and the shear force at the abutment. The selected traffic events were then used for transient dynamic analysis.

3 RESULTS

The results of the simulations were processed and DAF-value was evaluated for each traffic event. The DAF was evaluated separately for bending moment and shear force. In the next step, DAF-values of different quantiles were determined. In here, quantiles of 95%, 99% and 100% (the maximum) were evaluated from a group of traffic events. In order to capture the dependance between DAF and the magnitude of quasi-static load effects, the traffic events were first divided into 5 clusters based on the magnitude of quasi-static load effect. The cluster boundaries

were chosen on the basis of cluster size, with diminishing cluster size towards the high loading events. An example for one bridge is displayed in Figure 3, where the magnitude of quasi-static response is plotted on horizontal axis. $M_{q,st}/M_{Q,k}$ is the ratio between peak quasi-static bending moment during one traffic event to the bending moment due to load model LM1. Similarly, $V_{q,st}/V_{Q,k}$ is the ratio of peak shear force to the code-value. The green areas represent the magnitude of 95%-, 99%- and 100% DAF-quantiles of the respective cluster of simulated traffic events. In this example, which shows calculations on a reinforced-concrete slab with 15 m span, DAF-values in the highest cluster ($X_{q,st}/X_{Q,k} > 0.63$) reach values of $DAF_{95\%} = 1.082$ for bending moment and $DAF_{95\%} = 1.044$ for the shear force.

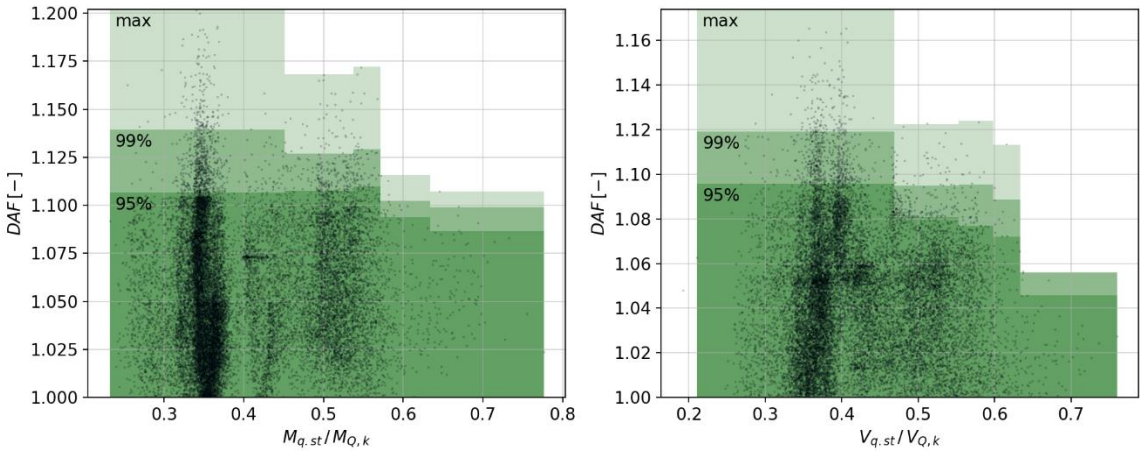

Figure 3: DAFs of traffic events on RC slab with 15 m span, μ=22.8 t/m, f_0=4.2 Hz. Bending moment (left) and shear force (right).

Figure 4 shows a similar evaluation on a composite bridge with welded steel girders with 50 m span. In here, the DAF-values in the highest cluster reach values of $DAF_{95\%} = 1.049$ for bending moment and $DAF_{95\%} = 1.04$ for the shear force.

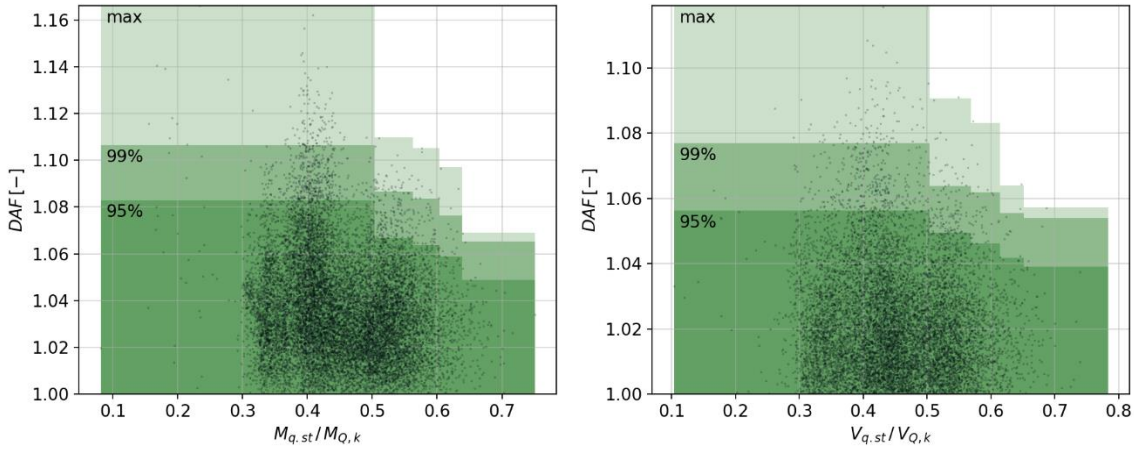

Figure 4: DAFs of traffic events on composite bridge with welded steel girders with 50 m span, μ=12.5 t/m, f_0=1.8 Hz. Bending moment (left) and shear force (right).

The lowest DAF values were achieved on long-span bridges. Figure 5 shows an evaluation on a steel box-girder bridge with 90 m span. In here, the DAF-values in the highest cluster reached values of $DAF_{95\%} = 1.021$ for bending moment and $DAF_{95\%} = 1.014$ for the shear force.

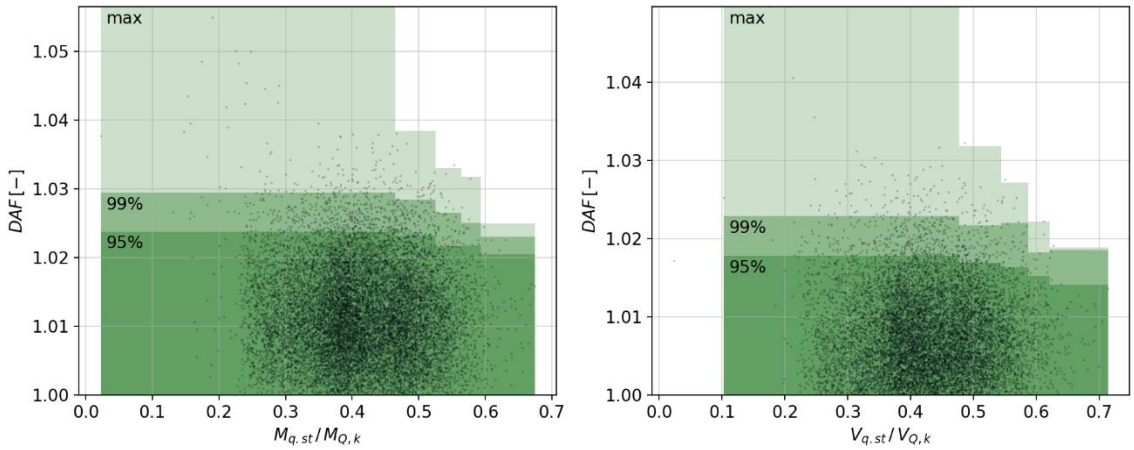

Figure 5: DAFs of traffic events on steel box-girder bridge with 90 m span, μ=7.7 t/m, f_0=1.4 Hz. Bending moment (left) and shear force (right).

A question that is not answered in this work is, which cluster of traffic events should be used and using which percentile of DAF-values of this cluster. The following figures show a different type of evaluation, which is considered to be a possible option for the choice of representative DAF-value. On the horizontal axis, portion of vehicles included in the evaluation is displayed. The vehicles are sorted by magnitude of the quasi-static bridge response, which means that for example in the portion of 0.001% (=10^{-5}), the highest 0.001% of all traffic events are included, in terms of the quasi-static bridge response. On the vertical axis, the maximum DAF (100%-quantile) within the respective group of events is plotted. The resulting curves show a step-wise characteristic, which is a natural consequence of evaluating the maxima of data with consecutively increasing group size. Figure 6 shows results of the same DAF-values that are also displayed in Figure 3.

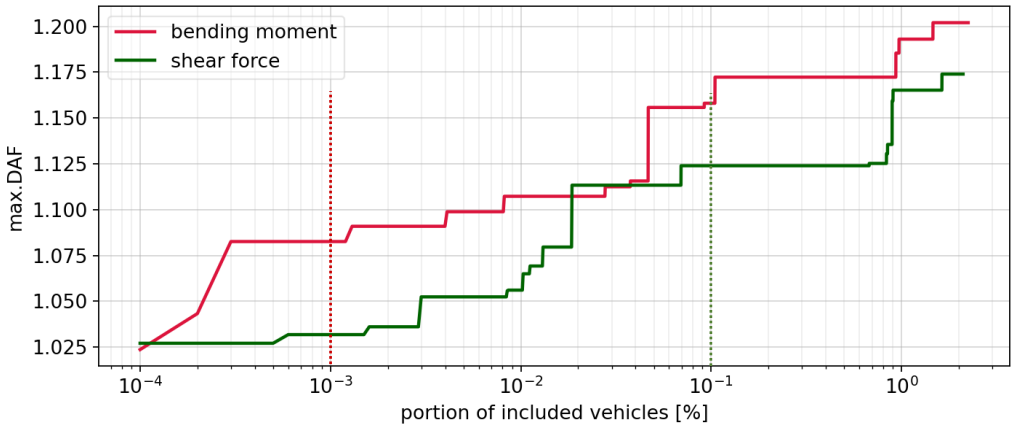

Figure 6: Maximum DAFs of traffic events on RC slab with 15 m span, μ=22.8 t/m, f_0=4.2 Hz with consecutively increasing size of traffic events group.

Figure 7 shows a similar evaluation of results on a steel bridge, which are also displayed in different form in Figure 5. In Figure 6 and Figure 7, two vertical dotted lines (one red, one green) are plotted. These mark the portions of vehicles, which were chosen for the results displayed in Figure 8. The red dotted line represents the portion of vehicles of q=10^{-5}; the green dotted line the portion of vehicles of q=0.001. These results are plotted in Figure 8 using red and green marks, respectively.

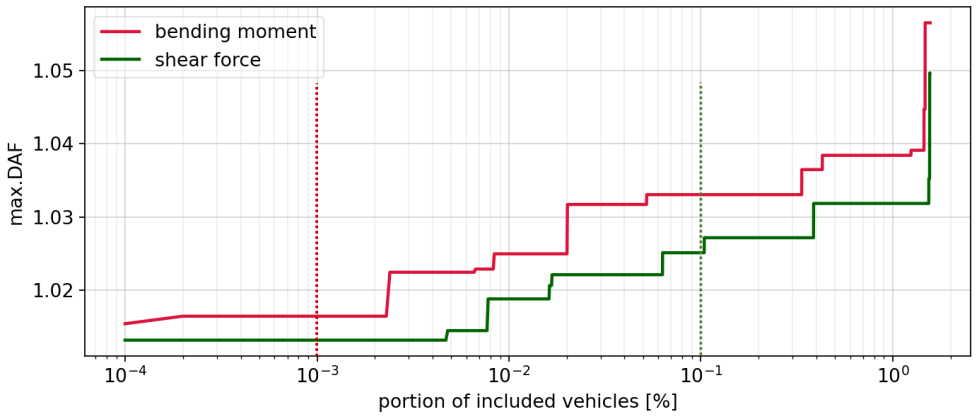

Figure 7: Maximum DAFs of traffic events on steel box-girder bridge with 90 m span, μ=7.7 t/m, f_0=1.4 Hz with consecutively increasing size of traffic events group.

Figure 8 summarizes results of evaluated maximum DAFs on all investigated bridges, using the portion of included vehicles of q=10^{-5} and q=0.001.

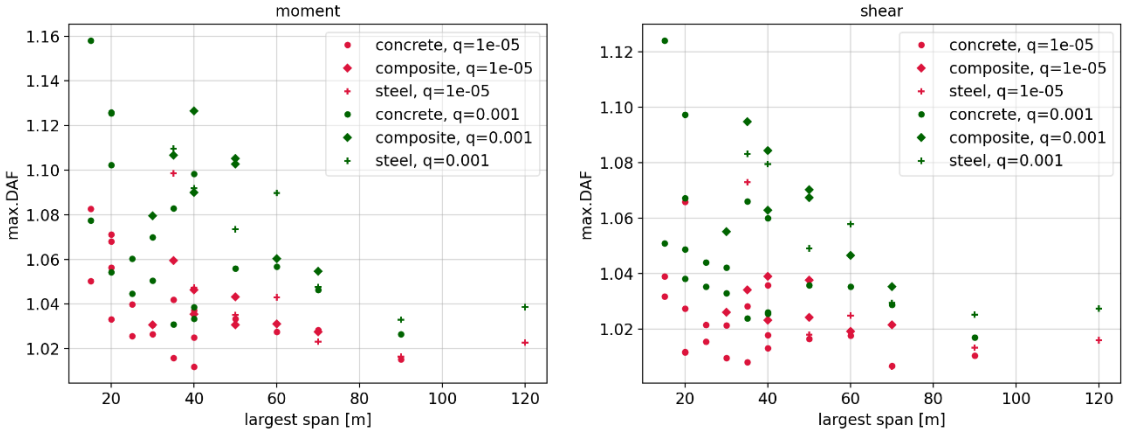

Figure 8: Maximum DAFs of traffic events on all investigated bridges, evaluated at portions of included vehicles of q=10^{-5} and q=0.001.

4 CONCLUSION

This paper presented results of dynamic amplification factors (DAFs) calculated on a chosen set of bridges, using simulated traffic flows that encompass 20 years of operation. Comparison of the resulting DAFs confirm results of other research works in that the DAF decreases with increasing magnitude of the quasi-static load effect. Further dependencies that were observed are the decrease of DAF-values with increasing span length, and the general tendency for higher DAF-values on lighter bridges (e.g. steel compared to composite and concrete bridges).

The resulting DAFs were evaluated for different quantiles of traffic events sorted by their quasi-static magnitude. A question that remains unanswered in this work is, which quantile should be chosen for the representative DAF value. This will be a topic in continuation of this research, where further statistical evaluations are planned, as well as the comparison of the evaluated DAFs to the Assessment Dynamic Ratios (ADRs), which were proposed by other research groups.

ACKNOWLEDGEMENTS

Authors thankfully acknowledge the funding of research projects LEVITATE within Horizon 2020 research and innovation programme under grant agreement No 824361; and research project REAL-LAST funded by FFG within Mobility of Future, project No FO999889387, which made this work possible.

REFERENCES

[1] European Committee for Standardization, EN 1991-2, Actions on structures – Part 2: Traffic loads on bridges, 2012.

[2] B. Hu, G. Brandstätter, M. Ralbovsky, M. Kwapisz, A. Vorwagner, R.d. Zwart, C. Mons, W. Weijermars, J. Roussou, M. Oikonomou, Ziakopoulos, A. Chaudhry, S. Sha, R. Haouari, H.C. Boghani, Medium-term impacts of cooperative, connected, and automated mobility on freight transport, *Deliverable D7.3 of the H2020 project LEVITATE*, 2021.

[3] J. Kalin, A. Žnidarič, A. Anžlin, M. Kreslin, Measurements of bridge dynamic amplification factor using bridge weigh-in-motion data. *Structure and Infrastructure Engineering, p.1164-1176,* 2022.

[4] E.J. O'Brien, D. Cantero, B. Enright, A. González, Characteristic Dynamic Increment for extreme traffic loading events on short and medium span highway bridges. *Engineering Structures 32*, p. 3827–3835, 2010.

[5] C. Carey, E.J. O'Brien, A. Malekjafarian, M. Lydon, S. Taylor, Direct field measurement of the dynamic amplification in a bridge. *Mechanical Systems and Signal Processing 85*, p. 601–609, 2017.

[6] U. Freundt, S. Böning, et.al.: Anpassung von DIN-Fachberichten „Brücken" an Eurocodes (Adaptation of DIN technical reports "Bridges" to Eurocodes), *Berichte der Bundesanstalt für Straßenwesen (Reports of the Federal Highway Research Institute), Brücken- und Ingenieurbau Heft B 77 (Bridges and Engineering Construction issue B 77)*, ISBN 978-3-86918-108-0, Bergisch Gladbach, Germany, 2011.